Stabilization of predissociating nitric oxide Rydberg molecules using microwave and radio-frequency fields

Elena Murgu, J. D. D. Martin[a), and T. F. Gallagher
Department of Physics, University of Virginia, Charlottesville, Virginia 22901

We present three techniques for suppressing predissociation of the nitric oxide Rydberg states normally excited in pulsed-field ionization zero-kinetic-energy photoelectron spectroscopy. By applying a combination of appropriate dc and microwave fields it is possible to inhibit predissociation by resonantly mixing Stark states of adjacent principal quantum number n, with similar parabolic quantum number k. Lifetime enhancement is also obtained by using an appropriate radio-frequency field to resonantly mix Stark states of the same n. Finally, in the absence of dc fields, microwaves are used to stabilize optically excited nf Rydberg states, by inducing transitions to higher angular momentum states with longer lifetimes, specifically to the $n \pm 1$, $l \geq 4$ states. © *2001 American Institute of Physics.* [DOI: 10.1063/1.1400788]

I. INTRODUCTION

The study of molecular Rydberg states is often complicated by a nonradiative decay mechanism not present in atoms, namely predissociation; for example, np Rydberg states approaching the first ionization limit of NO decay into N and O atoms. In this case, the $50p$ predissociation lifetime is estimated to be 0.4 ns,[1] five orders of magnitude shorter than the radiative lifetime of the $50p$ state of hydrogen, which is 23 μs.[2] Since both predissociation and radiative decay rates obey a n^{-3} scaling law, one can extend the lifetimes of Rydberg states simply by going to higher n. However, doing so introduces an increased sensitivity to the stray electric fields that are unavoidable in any experimental apparatus. A reflection of this sensitivity at high n is the significant lifetime lengthening of optically accessible Rydberg states that is often observed due to stray-field Stark mixing with longer-lived high-l states.[3,4] For detailed studies of molecular Rydberg state properties, such as those performed on atoms, it is desirable to work at lower n, where l remains a good quantum number under typical experimental conditions, and specific nl states can be selectively excited.

For example, the quantum defects of high-l, nonpenetrating Rydberg states can provide information on the electronic properties of the ionic core, such as the dipole polarizability, and quadrupole moment. Sturrus *et al.*[5] have demonstrated that microwave spectroscopy of the higher angular momentum states of $n=10$ Rydberg states of H_2 is a sensitive test of electronic structure calculations for the H_2^+ ion. This type of measurement has not been extensively applied to molecules, other than hydrogen, primarily because of difficulties in exciting long-lived, low-n molecular Rydberg states. The short lifetimes of optically accessible molecular Rydberg states can also restrict the application of the very high resolution millimeter wave spectroscopy recently developed by Osterwalder and co-workers.[6,7]

Thus there is strong motivation for developing techniques for stabilizing low-n Rydberg states against decay. In previous work, we demonstrated that microwaves can stabilize the predissociating np series of NO as low as $n \approx 70$.[8] However, at this n our laser bandwidth limited the observation of individual n states. In this paper, we demonstrate that this technique can be extended to the regime where n states can be optically resolved with our excitation lasers and describe alternative approaches to effecting stabilization of the Rydberg states.

II. RYDBERG STATES OF NO

There are three features of NO that make it an attractive system for the development of experimental techniques associated with molecular Rydberg states. First, the spectroscopy is well known. Second, it can be excited from its ground state to the vicinity of its ionization potential using a double-resonance excitation scheme involving only two frequency-doubled dye lasers. Finally, Rydberg states of NO are convenient because the ground state ion, NO^+, has a $^1\Sigma$ electronic structure, simplifying the analysis of its coupling with the Rydberg electron.

Rydberg states of NO have received substantial attention in the context of pulsed-field ionization zero-kinetic-energy photoelectron (PFI-ZEKE) spectroscopy.[9,10] This technique was first demonstrated using NO,[11] and there have been several subsequent studies.[4,12–14] The majority of these experiments are based on an excitation scheme similar to the one described in this paper: After laser excitation to a specific rovibrational level of the $A\,^2\Sigma^+$ state, the NO molecules are excited to the vicinity of the ionization threshold by a second laser. In this excitation scheme, only certain Rydberg series of specific orbital angular momentum l are optically bright. This l selectivity will now be discussed.

If the first laser excites a $N=0$ rotational level of the $A\,^2\Sigma^+$ state—as is the case in this and several of the other experiments—the reasoning is straightforward: By dipole selection rules, only final states with total angular momentum of $J=1$ will be excited. This total angular momentum of the final Rydberg state can be described as the coupling of the

ionic core and Rydberg electron angular momenta: N^+ and l, respectively (neglecting spin). Under this assumption, Rydberg states approaching the $N^+=0$ ionization threshold must have $l=1$. In other words, only the np series will be optically bright. By the same angular momentum conservation rule, Rydberg states approaching $N^+=1$ are constrained so that $0 \leq l \leq 2$. Likewise, Rydberg states approaching $N^+=2$ must satisfy $1 \leq l \leq 3$. The optically active $3s\sigma$ electron of the intermediate state has a small amount (5%) of d character, and is primarily *gerade*-like with only 0.3% p character.[15] Thus for both $N^+=0$ and $N^+=1$ only the np series is accessible, whereas both np and nf series approaching $N^+=2$ are accessible (see, for example, Ref. 4).

Both the np and nf series of NO are known to predissociate: Following excitation they decay predominantly into free neutral atoms, with the kinetic energy of these fragments taking up any excess energy. Vrakking and Lee[4] have determined that for the np ($N^+=0$) series, the predissociation rate is (in atomic units) $1/\tau_p = 4.6 \times 10^{-2}/(2\pi n^3)$ and for the nf ($N^+=2$) series it is $1/\tau_f = 1.2 \times 10^{-3}/(2\pi n^3)$. At $n=200$, typical of PFI-ZEKE spectra in the literature,[11] this gives a np-series predissociation lifetime of 160 ns. Thus, as Chupka pointed out,[3] the observation of a field ionization signal tens of microseconds after photoexcitation is surprising—one would expect these states to have decayed by this time. The other $l \leq 3$ states also have short lifetimes. Based on previous experimental data, the ns and nd series have estimated decay rates of $1/\tau_s = 1.4 \times 10^{-2}/(2\pi n^3)$, and $1/\tau_d = 2.9 \times 10^{-2}/(2\pi n^3)$, respectively.[16] However, the predissociation rate drops dramatically with increasing l, since the Rydberg electron is kept away from the ionic core by the centrifugal barrier. For example, the $55g$ state has a lifetime of approximately 1 μs.[17] Assuming an n^{-3} scaling of the predissociation rate implies a lifetime τ_g given by $1/\tau_g = 3 \times 10^{-5}/(2\pi n^3)$. States of higher l are expected to have even lower predissociation rates, but these states are normally not optically accessible. Nonetheless, at the very high n typical of PFI-ZEKE, Rydberg states are highly susceptible to the influence of stray fields, and as proposed by Chupka,[3] the mixing of the optically accessible low-l states with the long-lived high-l states can "dilute" the decay rate, so as to lengthen lifetimes, explaining the PFI-ZEKE results.

It is useful to have simple rules for when low-l states become mixed with the Stark manifold of high-l states. To help illustrate some of the following points, Fig. 1 shows a calculated Stark map for $m=0$, that is, the energy levels of NO as a function of electric field. To a good approximation, the energy of an nl state in zero field relative to the ionization limit is

$$W = -\frac{1}{2n^2} - \frac{\delta_l}{n^3},\tag{1}$$

where δ_l is the quantum defect of the l series.

In an electric field F the energy of the extreme red (blue) $m=0$ Stark states is approximately

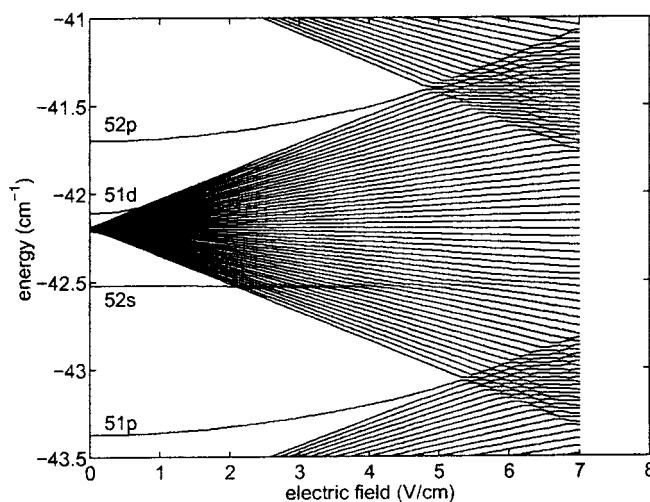$$W = -\frac{1}{2n^2} - (+) \frac{3n^2 F}{2}.\tag{2}$$

FIG. 1. Calculated Rydberg state energy levels of NO as a function of electric field strength for $m=0$, in the vicinity of $n=51$. This calculation was performed in the manner described by Zimmerman *et al.* (Ref. 39) and neglects coupling to Rydberg series approaching other ionization thresholds [see Vrakking (Ref. 1)]. The quantum defects used for this calculation are listed in Table I.

From Eqs. (1) and (2), an extreme Stark state of a given n will meet the nearest member of a Rydberg series of low angular momentum l when the field satisfies

$$F = \frac{2|\Delta_l|}{3n^5},\tag{3}$$

where $\Delta_l = \delta_l - q$, and q is the integer closest to δ_l. Rewriting in laboratory units:

$$F \approx 3.43 \times 10^9 \frac{|\Delta_l|}{n^5} \quad \text{V/cm}.\tag{4}$$

Once the low-l state intersects with an extreme Stark state, its l character begins to mix throughout the manifold. Equation (3) gives the threshold field at which this occurs. However, this formula is clearly a simplification, since the polarizability of the low-l state is neglected, but it does allow one to make simple estimates and contains the proper scaling.

As an example, for the np series of NO: $\delta_p = 0.7$ and $\Delta_p = -0.3$. Vrakking and Lee[4] have shown experimentally that the lifetime of states in the optically accessible np series increases dramatically if one applies a field above the "critical" field: $F = (6 \times 10^8)/n^5$ V/cm, in rough agreement with Eq. (3). They also studied the nf ($N^+=2$) series and found that due to its lower quantum defect ($\delta_f \approx 0.01$) it requires a correspondingly smaller dc field to have its lifetime significantly lengthened. For later reference, quantum defects and decay rates for the lowest-l states of NO are listed in Table I. These change slightly depending on the ion-core state,[4] but are sufficiently accurate for estimating various quantities throughout this paper.

Although the electric field makes longer-lived states optically accessible, the disadvantage of using it for stabilization is that the coupling to lower-l states still allows predissociation to occur. This suggests the following compromise: Excite the Rydberg states in the presence of a dc field, then switch it off, with the hope of moving part of the population

TABLE I. Quantum defects and decay rates of the low-l states of NO, based on Table II of Bixon and Jortner (Ref. 16). The g-series quantum defect listed has not been determined spectroscopically, but was estimated based on the long-range force model of Jungen and Miescher (Refs. 37 and 38) using the same constants as Fujii and Morita (Ref. 17). The atomic unit of time is approximately 2.42×10^{-17} s.

l	δ_l	$1/\tau_l$ (a.u.)
s	1.2	$0.014/(2\pi n^3)$
p	0.7	$0.046/(2\pi n^3)$
d	-0.05	$0.029/(2\pi n^3)$
f	0.01	$0.0012/(2\pi n^3)$
g	0.003	$0.00003/(2\pi n^3)$

into higher-l states during the process. Since high-l states do not predissociate, this removes the drain present when a static field is used. Held *et al.*[14] provided a demonstration of this by Stark-mixing the optically bright nf ($N^+ = 2$) Rydberg series of NO with the higher-l manifold during photoexcitation, and then switching it off. Their resulting PFI-ZEKE spectrum showed a dramatic enhancement in Rydberg state signal. Recently there have been two other proposals for stabilization of Rydberg states following photoexcitation using time-dependent fields made by Ivanov and Stolow[18] and Bellomo and Stroud.[19]

In previous work we demonstrated an alternative technique for stabilization of optically accessible Rydberg states of NO using resonant mixing by microwave fields.[8] This suppression of predissociation enhances the PFI-ZEKE spectra in a significantly different manner from that observed by Held *et al.*[14] In particular, enhancement is observed over a small, controllable range of n's for which the microwave angular frequency ω matches the $n \rightarrow n+1$ energy spacing:

$$\omega = 1/n^3, \tag{5}$$

producing a resonance in the PFI-ZEKE spectrum at a well-defined energy below the ionization limit:

$$W = -\frac{\omega^{2/3}}{2}, \tag{6}$$

as experimentally demonstrated in Ref. 8. For reference, this is rewritten in laboratory units

$$W \approx -(f/0.181)^{2/3} \text{ cm}^{-1}, \tag{7}$$

where f is the microwave frequency (in GHz).

This microwave coupling took place in the presence of a static field on the order of the Inglis–Teller field[20] for the approximate n that is enhanced. The observed data suggest that the microwave coupling drives transitions between Stark states of nearly equal parabolic quantum number k. This repetitive cycling eventually spreads population throughout the entire manifold to regions that are optically inaccessible in zero field, but where the lifetimes are much longer. In this paper, additional experimental evidence is provided to support this hypothesis.

III. EXPERIMENT

The experimental setup was similar to that presented in Ref. 8. A $1+1'$ multiphoton excitation scheme was used to excite supersonically cooled NO molecules to the vicinity of the first ionization threshold. A pulsed nanosecond dye laser was frequency doubled to produce light (≈ 225 nm) that excited the NO molecules to the $A\,^2\Sigma^+$, $v = 0$, $N = 0$ intermediate state from the $X\,^2\Pi$, $v = 0$, f_2 ($K = 2$) level (using the same notation as Engleman *et al.*,[21] except K is replaced by N for the $A\,^2\Sigma^+$ state, to conform to common usage). This transition is at 44 074.1 cm^{-1}, that is, the O_{12} ($K = 2$) line of Table III of Ref. 21. The energy of the $A\,^2\Sigma^+$, $v = 0$, $N = 0$ intermediate state relative to the lowest state of the molecule $X\,^2\Pi$, $v = 0$, f_1 ($K = 0$) is 44 198.92 cm^{-1} [i.e., the $Q(1)$ line of Table III of Ref. 21). Once in the $A\,^2\Sigma^+$ state, a second frequency-doubled dye laser excited the molecules to energies in the vicinity of the first ionization threshold. Spectra that were taken as a function of this laser energy were calibrated using uranium lines observed at the fundamental wavelength by the optogalvanic effect in a hollow cathode discharge.[22] The spectra are displayed using an energy scale relative to the field-free $N^+ = 0$ ionization threshold, by subtracting the first ionization threshold energy from the calibrated second laser photon energy. By combining the first ionization threshold relative to the lowest state of the molecule of 74 721.67±0.10 cm^{-1} (due to Biernacki *et al.*[23]), with the $A\,^2\Sigma^+$, $v = 0$, $N = 0$ state energy of 44 198.92 cm^{-1} discussed above, this threshold energy is computed to be 30 522.75±0.1 cm^{-1}. However, Vrakking and Lee[4] quote 30 522.44 cm^{-1} for this quantity, with an estimated accuracy better than 0.1 cm^{-1}.[24] By extrapolating a nf Rydberg series observed in our spectra (*vide infra*) a value of 30 522.45±0.2 cm^{-1} is found for this quantity, in closer agreement with the Vrakking–Lee work.[4]

The molecular beam and two laser beams crossed halfway between two parallel aluminum plates separated by 1.27 cm. A field ionization pulse of 630 V/cm, with a rise time of roughly 100 ns, was applied using these plates, approximately 750 ns after photoexcitation, and the electrons from field ionization were extracted through a mesh-covered hole in the upper plate to a microchannel plate detector. Electrons, due to this field ionization pulse, if any, were selectively detected with a gated integrator, so that prompt photoelectrons, and electrons due to autoionization did not contribute to the observed signal. Scanning the photon energy resulted in a PFI-ZEKE spectrum of NO similar to those obtained in previous studies[13] [see Fig. 2(a)]. The observed signal corresponds to the electric field ionization of Rydberg states approaching the different ionization thresholds of the molecule. Over this energy range, these thresholds correspond to leaving an ion core with different amounts of rotational energy.

The energy spacings of the different rotational thresholds should correspond to the rotational energy level spacings of the ion, and may be determined using the spectroscopic information summarized in Ref. 25: $E(N^+ = 1) - E(N^+ = 0) = 4.0$ cm^{-1}, and $E(N^+ = 2) - E(N^+ = 0) = 11.9$ cm^{-1}. These are marked in Fig. 2.

The magnitude of the pulsed field dictates the lowest n that may be field-ionized. In the work presented herein, the signal on the low-energy side of the spectra is dictated by the lifetimes of the lower-n Rydberg states[13]—the states decay before they can be field ionized. For example, in this case, a

J. Chem. Phys., Vol. 115, No. 15, 15 October 2001

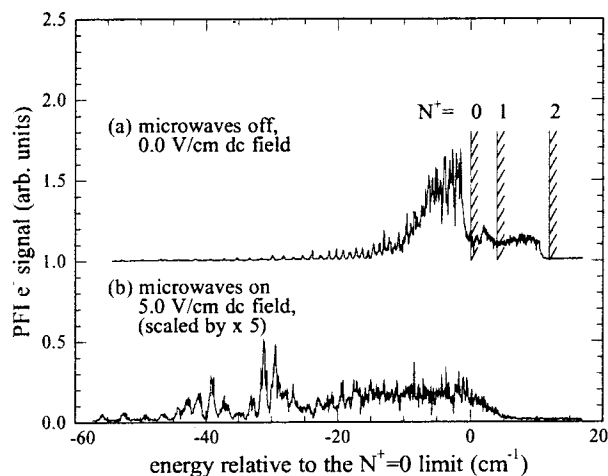Nitric oxide Rydberg molecules   7035

FIG. 2. PFI-ZEKE spectra of NO taken (a) without microwaves, 0 V/cm dc field, and (b) with a microwave field of 51 GHz and 1.0 V/cm amplitude on during photoexcitation, and switched off approximately 10 ns afterwards, 5 V/cm dc field. This has been increased in vertical scale by a factor of 5 for easier comparison with (a).

field-ionization voltage of 600 V/cm should be sufficient to efficiently field-ionize all Rydberg states with $n > 40$, even assuming diabatic ionization.[20] However, the spectrum without microwaves present shows no evidence of field ionization of $n = 40$ Rydberg states approaching the first threshold—they have decayed during the 750-ns waiting period following photoexcitation.

In this paper, several techniques are demonstrated for enhancing this PFI-ZEKE spectrum using microwave and radio-frequency fields. In all cases, the introduction of the microwave field causes population transfer, from the optically bright, rapidly decaying Rydberg states to longer-lived states.

To cover the frequency range 26.5–60 GHz, two active frequency multipliers were used. These devices generate harmonics of the source frequency and amplify them (in this case a 0.01–20-GHz Hewlett-Packard 83620A sweep oscillator). Both multipliers were located inside the vacuum chamber, and were water-cooled. To turn the generated microwaves on and off, we modulated their inputs at the fundamental frequency by using either the external pulse modulation input of the sweep oscillator (50 ns rise/fall times), or an external switch (Hewlett-Packard 11720A, 10 ns rise/fall times).

Microwaves from 26.5 to 40 GHz were generated using an active doubler (Avantek, AMT-400X2-31). The output port of this device is a WR28 waveguide flange. A horn was mounted on this flange that flares out from the WR28 dimensions (0.711 cm×0.356 cm) to 2.4×1.8 cm over 4 cm. The open end of this horn was directed towards the region where the laser and molecular beams cross—located 4 cm from the end of the horn. As a crude estimate of microwave intensity in the interaction region, we divided the total power of the device by the area that the microwave horn opening would be if extended to the interaction region, in this case 13 cm².

Microwaves in the frequency range of 40–60 GHz were obtained using an active quadrupler (Narda/DBS Microwave,

DBS-4060×410). The output port of this device is a WR19 flange. A horn was mounted on this flange that flares out from the WR19 dimensions (0.478 cm×0.239 cm) to 1.5 ×1.0 cm over 2.7 cm. The open end of this horn was directed towards the laser beam molecule interaction region—located 4 cm away from the end of the horn. As a crude estimate of microwave intensity in the interaction region, we divided the total power of the device by the area that the microwave horn opening would be, if extended to the interaction region, in this case 6 cm².

Radio-frequency fields from 25 to 150 MHz were applied using the same plates above and below the ionization region that were used to apply dc fields and the field ionization pulse.

IV. MICROWAVE RESONANT ENHANCEMENT WITH A dc ELECTRIC FIELD

With microwave sources covering 26.5–60 GHz the work described in Ref. 8 was extended to lower n. Figure 2(b) shows a PFI-ZEKE spectrum of NO, modified by the introduction of a microwave field of 51 GHz, switched off approximately 10 ns after photoexcitation. In addition, a static electric field of 5 V/cm was present (parallel to the microwave field polarization). The set of microwave-induced resonances observed at lower n will be discussed first. From Eq. (7), the resonant enhancement is expected to occur 43 cm^{-1} below the ionization threshold (at $n \approx 50$). As Fig. 2(b) shows, a set of peaks centered around this energy is observed. The energy spacings of these peaks match those of a Rydberg series approaching the $N^+ = 0$ ionization threshold. Thus, these are interpreted as the excitation of particular n's that are stabilized against predissociation. Molecules that are excited, and would normally decay, are transferred to states that live long enough to be field-ionized 750 ns after photoexcitation.

As was discussed in Sec. II, the optical excitation scheme used in this experiment only allows access to the p series approaching $N^+ = 0$. Given a quantum defect of 0.7 (Ref. 4), a field of 3.0 V/cm is sufficient for states of $n \geq 50$ to meet the manifold. It is clear that not all of the manifold becomes equally bright at this field, since this would imply that the adjacent n states would not be resolvable. This supports the assertion made in Ref. 8, that for effective stabilization, only part of the manifold is optically bright and quickly decaying. The microwave field then causes a spreading, or percolation, throughout the manifold to states that are longer-lived.

To have percolation of population from bright to dark states, *and* maintain the resonance condition $\omega = 1/n^3$, requires that transitions occur between states of $\Delta n = 1$ and $\Delta k \approx 0$. The quantum number k is defined through the energy level expression

$$W = -\frac{1}{2n^2} + \frac{3}{2}nkF \qquad (8)$$

(which is only rigorous for hydrogen). We have calculated the dipole moments of the $n = 51$ to $n = 52$ ($m = 0$) transitions as a function of k using Eqs. (65.1) and (65.3) of Bethe
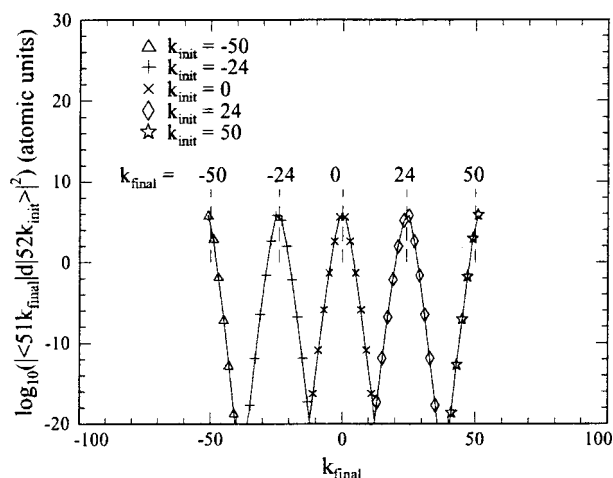
FIG. 3. Dipole matrix elements between $n=50$ and $n=51$, $m=0$, hydrogenic Stark states for different initial Stark quantum numbers $k_{initial}$, as a function of the final quantum number k_{final}. This illustrates the strong propensity rule: $\Delta k = \pm 1$.
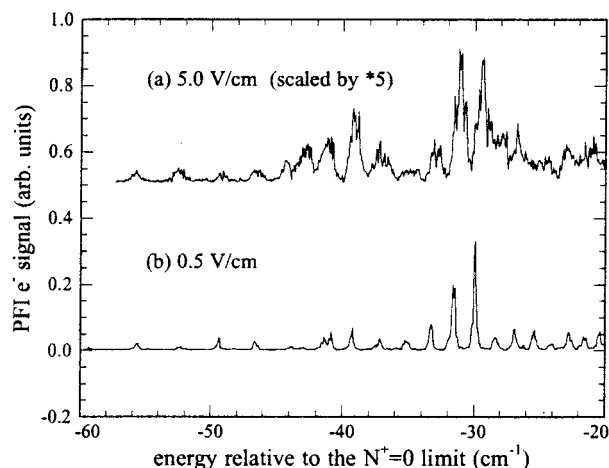

FIG. 4. PFI-ZEKE spectra of NO in the presence of a 51 GHz, 1.0 V/cm amplitude microwave field, switched off 10 ns following photoexcitation, both with (a) 5.0 V/cm dc field and (b) 0.5 V/cm dc field. The spectrum taken in a 5.0 V/cm field has been increased in vertical scale by a factor of 5.

and Salpeter[2] with the result shown in Fig. 3. By far the largest dipole matrix elements correspond to $\Delta k = \pm 1$ (which also holds for $m \neq 0$). This is precisely the dependence required to have both percolation and a well-defined resonance when $\omega = 1/n^3$.

A second distinct set of enhanced peaks is observed at approximately 30 cm^{-1} below the $N^+ = 0$ ionization threshold in Fig. 2(a). Since these peaks are separated from the lower set of peaks by roughly the $E(N^+=2)$, $E(N^+=0)$ rotational energy level spacing of the ion, it is reasonable to assign them as enhanced Rydberg states of $n \approx 50$ converging to the $N^+ = 2$ ionization threshold. Note that the spacing between peaks is the same at 30 and 43 cm^{-1} below the first ionization threshold. In Ref. 8 we were unable to observe clear enhancement of Rydberg states approaching the $N^+ = 2$ threshold due to the presence of the strong nonresonant PFI-ZEKE signal approaching the first ionization threshold, which was located in the same energy range as the expected enhancement approaching the $N^+ = 2$ threshold.

In principle, the enhancement of the p Rydberg series approaching the $N^+ = 1$ threshold should be observed as well. However, in practice the transition strengths to this series are relatively weak in comparison to the np series approaching the $N^+ = 0$ threshold, making enhancement more difficult to observe (in low pulsed field PFI-ZEKE spectra, where the $N^+ = 0$ and $N^+ = 1$ lines may be spectrally resolved, the $N^+ = 1$ line is roughly four times weaker than the $N^+ = 0$ line; see Fig. 3 of Ref. 13).

In the work at higher n reported in Ref. 8, it was emphasized that in order to observe enhancement at the quoted microwave powers, a static field was required as well. It was also noted that this static field had an Inglis–Teller-type scaling (i.e., $F \propto 1/n^5$). Figure 4 shows an enlarged version of the spectra in Fig. 2(b), taken at two different static fields. When the dc field was reduced from 5.0 to 0.5 V/cm, the enhancement of the Rydberg series approaching $N^+ = 0$ was greatly reduced, whereas the series approaching $N^+ = 2$ became

sharper. From Sec. II, it will be recalled that an nf Rydberg series approaching the $N^+ = 2$ core is optically accessible. However, the only series approaching the $N^+ = 0$ threshold that is optically accessible is the np series. At a field of 0.5 V/cm a $50p$ Rydberg state has not met the high-l manifold yet. Thus, the field condition for mixing the optically bright state with longer-lived states in the manifold is not met, and as a result, no enhancement is seen approaching the $N^+ = 0$ threshold. However, a $50f$ state with a quantum defect of 0.01 will be mixed into the manifold by a field of 0.1 V/cm. Therefore at 0.5 V/cm this optically bright state provides a gateway into the Stark manifold, allowing lifetime lengthening by resonant mixing to occur. A larger field of 5.0 V/cm reduces the enhancement because all low-l states of $l \leq 3$ will be mixed into the manifold, as shown in Fig. 1, acting as drains when the microwave coupling is present. In addition, as one progresses to higher fields, once the initial interaction of the nf state and the manifold has occurred, the f character becomes successively more spread throughout the manifold, increasing the lifetime homogeneity, reducing the effective lifetime when microwave coupling is present.

The above discussion has emphasized the importance of the magnitude of the dc field used. However, in an analogous experiment on the resonant enhancement of dielectronic recombination of Ba^+ and e^- from a continuum of finite bandwidth, Klimenko and Gallagher[26] have found that the dc field requirement is removed if the microwave field amplitude F_{MW} is strong enough ($F_{MW} > 1/n^5$). We have also observed that in some of our spectra the dc field is not required if the microwave field is strong enough. However, because of the uncertainty in calibration of the microwave field strength in the interaction region, we were not able to verify the $F_{MW} > 1/n^5$ scaling.

Thus far we have discussed how a microwave field with a frequency that matches the $n \rightarrow n+1$ spacing can encourage population to spread to the longer-lived states in the manifold. This raises the question of whether or not percola-
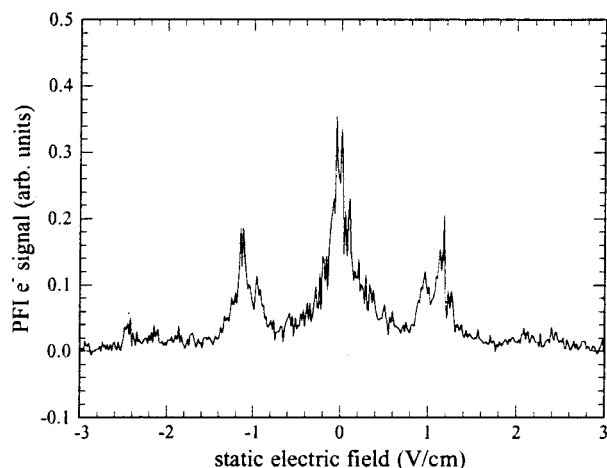
FIG. 5. Pulsed-field ionization signal from $n=54$ ($N^+=2$) and $n=65$ ($N^+=0$), 750 ns following photoexcitation as a function of dc field strength, in the presence of a rf field of 117 MHz, 0.25 V/cm amplitude, switched off 100 ns following photoexcitation.

tion can be induced *without* changing n. In other words: Can the Rydberg state signal be enhanced by driving transitions between Stark states of the same n?

To answer this question, rather than scanning the frequency of an applied field while setting the lasers to excite a specific n state with a fixed dc field strength, the following approach was taken: the laser was tuned to excite a $54f$ ($N^+=2$) Rydberg state, with a rf frequency of 117 MHz present, switched off 100 ns following photoexcitation, and the applied dc field strength was scanned between successive laser shots (see Fig. 5). The observed signal shows peaks at 0, 0.95, and 1.13 V/cm.

The enhancement at zero dc field will be discussed later. The stronger of the two nonzero field resonances occurs at 1.13 V/cm. At 1.13 V/cm, the spacing of adjacent k states of $n=54$ is 232 MHz. This is essentially twice the applied rf frequency of 117 MHz, suggesting that the adjacent Stark states in the manifold are resonantly coupled by two-photon transitions. This process spreads population throughout the manifold, from bright to dark states, leading to enhancement of the field ionization signal.

The smaller resonance at $F=0.95$ V/cm corresponds to the resonant mixing of Stark states approaching the $N^+=0$ ionization limit. A $54f$ ($N^+=2$) state is at roughly the same energy as $n\approx65$ ($N^+=0$). At $n=65$, $F=0.95$ V/cm, the spacing between adjacent Stark states of the same m is 235 MHz—almost exactly twice the applied rf frequency of 117 MHz.

By increasing the power of the rf used, it is also possible to induce higher-order multiphoton transitions (see Fig. 6). Resonances occur when the angular frequency ω satisfies

$$p\omega = \frac{3nF}{2},\qquad(9)$$

where $p=1,2,3,\ldots$, F is the static field strength, and n is the principal quantum number. Rewriting in laboratory units [F in V/cm and $f=\omega/(2\pi)$ in MHz]:

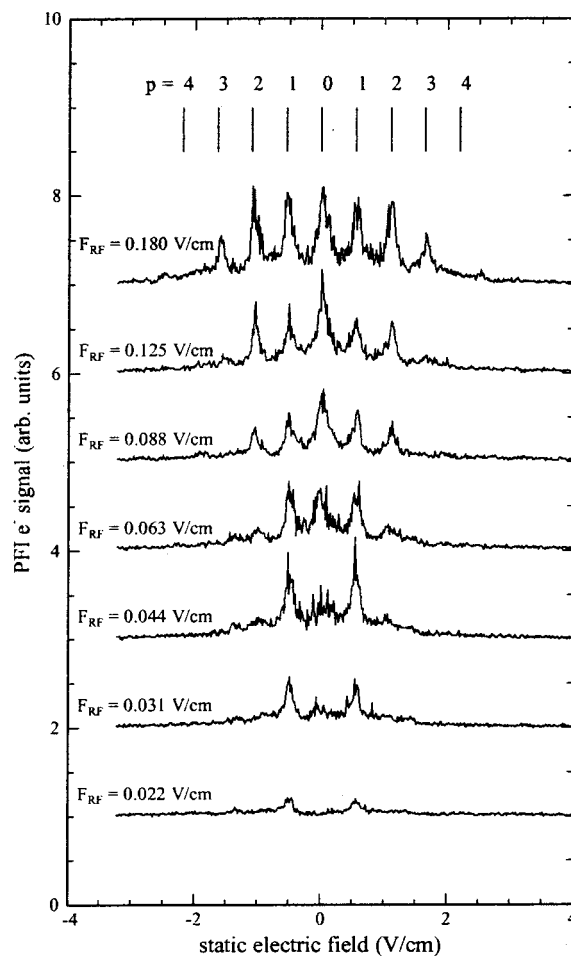$$pf \approx 1.919nF.\qquad(10)$$

FIG. 6. Pulsed-field ionization signal, from $n=48$ ($N^+=2$), 750 ns following photoexcitation as a function of dc field strength, in the presence of a rf field of 50 MHz, with varying amplitudes (indicated on the plot), switched off 100 ns following photoexcitation. These traces have been offset vertically for clarity. The labeled vertical lines indicate the expected positions calculated using Eq. (9).

By varying the laser excitation energy this relationship has has been verified for $n=48$ and $n=54$ (see Fig. 7). Agreement is to within one-tenth of the width of the observed resonances.

It is noted that all observed resonances correspond to the absorption of an even number of rf photons. For example, no one-photon resonances were observed. Such behavior is expected in a hydrogen atom, since its Stark states of the same n are not electric dipole coupled, to first order. The lowest-order coupling between such states is a two-photon coupling using $n\pm1$ states as virtual intermediate states. The existence of this second-order coupling allows microwave ionization of H and H-like states to occur through the extreme red Stark states.[27,28] The close agreement of the observed resonances with hydrogenic spacings is surprising in the case of NO.

Since the length of the excitation laser pulse was shorter than the rf period, it is appropriate to assume photoexcitation occurred in a certain field: a field that was a combination of the static and oscillating field. The exact value of this combined field would depend on the phase of rf, a parameter that was not controlled in these experiments. In fact, the rf phase
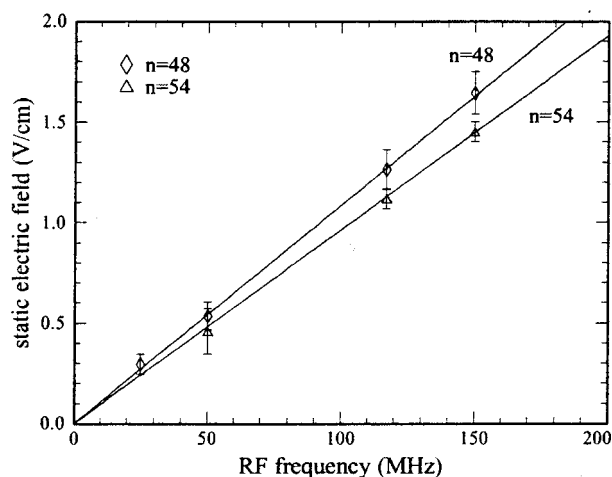
FIG. 7. Observed resonance positions in dc field scans, similar to those in Fig. 6 for optical excitation of both $n=48$ ($N^+=2$) and $n=54$ ($N^+=2$) in the presence of different rf frequencies. The solid lines indicate the theoretical positions [from Eq. (9) with $p=1$]. Error bars indicate the widths of the observed resonances, which are overestimates of the errors.
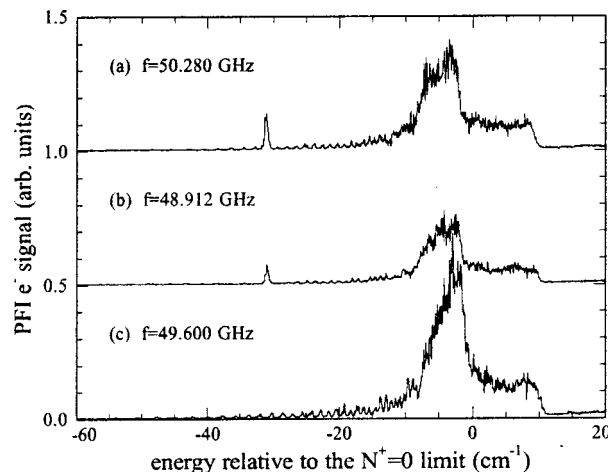

FIG. 8. PFI-ZEKE spectra with no dc field, in presence of microwave fields of approximately 0.1 V/cm amplitude, switched off 100 ns following photoexcitation, with frequencies of (a) 50.280 GHz, (b) 48.912 GHz, and (c) 49.600 GHz.

varied randomly from one laser shot to another. The change of the rf phase following photoexcitation will cause the total applied field to change. At certain values of the total applied field, the zero-field basis f state undergo avoided crossings with the Stark states. If these crossings are transversed rapidly (diabatically), the character of the states remains unchanged. However, if the crossings are traversed slowly (adiabatically), the l character of the population will change allowing stabilization to occur. How much population transfer occurs depends on the rate at which this crossing is traversed, and the magnitude of the energy gap at the avoided crossing.[29] Completely adiabatic traversal, while allowing stabilization, cannot, however, explain the experimentally observed resonances. These resonances are most likely due to traversals that are nonadiabatic. In other words, they are neither purely diabatic nor adiabatic. In this case, the results of multiple rf cycles constructively interfere to create the observed resonance phenomena.

The importance of the avoided crossings in stabilization is experimentally supported by the rf field strength scaling of the enhancement peak observed in Fig. 6 at zero dc field (i.e., the "resonance" in the center). Enhancement at zero dc field occurs over a broad range of n (down to at least $n=40$) and is not particularly frequency sensitive; it was observed at both 50 and 117 MHz. To further study this process, we examined its rf power dependence. With an rf frequency of 50 MHz at $52f$ ($N^+=2$), the enhanced signal goes from 20% to 80% of its maximum as the rf field is increased from 0.04 to 0.07 V/cm. For comparison, it is noted that the threshold dc field for mixing the $51f$ into the manifold is roughly 0.09 V/cm. For $39f$ ($N^+=2$), the enhanced signal goes from 20% to 80% of its maximum as the rf field is increased from 0.1 to 0.2 V/cm, and the threshold for mixing this state into the manifold is 0.4 V/cm. Because of the uncertainty in the efficiency of the rf coupling, these field strength estimates could be in error by as much as a factor of 2. However, these results strongly suggest that the rf field

must be sufficient to reach the first avoided crossing of the f state with the manifold.

Further experimental studies will concentrate on the calibration of the field strength, and a more precise control over the timing of the field. Specifically, varying the phase of the rf field at photoexcitation, how long the field is present, and how it is switched off could have dramatic effects on how much of the population is transferred to long-lived regions of the manifold and, consequently, the observed signal due to field ionization after the waiting period. A more detailed explanation would likely profit from the application of Floquet theory, an approach found to be useful in determining the influence of these factors on rf induced transitions between atomic Rydberg states.[30]

From the practical point of view, this rf enhancement technique does not require sophisticated equipment, and could be implemented in many PFI-ZEKE and mass-analyzed threshold ionization (MATI) spectrometers with minor modifications.

V. MICROWAVE RESONANT ENHANCEMENT WITH NO dc ELECTRIC FIELD

The preceding discussion concentrated on extending Rydberg state lifetimes by transferring population between Stark states. However, we would expect that in zero dc electric field, the highest-l states would have lifetimes exceeding those of any Stark states. Thus, it is of interest to investigate techniques for population transfer from the optically accessible low-l states to the long-lived high-l states in the *absence* of applied dc fields.

Figure 8(a) demonstrates that introducing a 50.280 GHz microwave field switched off 100 ns after photoexcitation, enhances the observation of a single Rydberg state, with no deliberate static field applied. The enhancement occurs at the energy of the $51f$ state converging to the $N^+=2$ threshold. If the laser frequency is tuned to the resonance observed in Fig. 8(b), and the microwave frequency is scanned, two resonances in the pulsed-field ionization signal are observed (see Fig. 9) at 48.92 and 50.40 GHz.
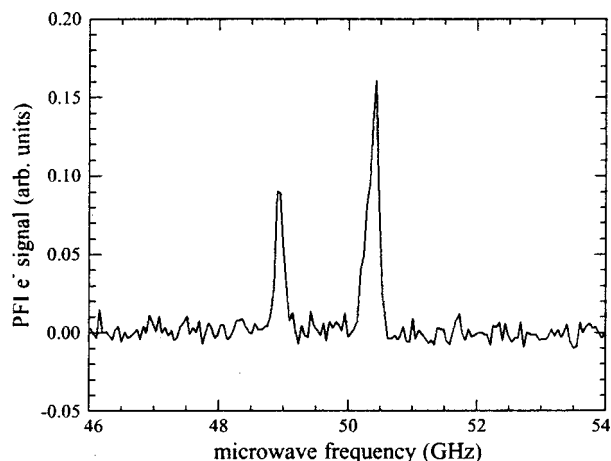
FIG. 9. Microwave-enhanced PFI-ZEKE signal at $51f$, as a function of frequency. Conditions are identical to Fig. 8.

TABLE II. Transition frequencies for stabilizing the optically excited nf ($N^+=2$) Rydberg series of NO. These were obtained from scans similar to the one shown in Fig. 9. The uncertainty in the l character of the final state is denoted by using k (which loosely refers to the Stark manifold). A down transition was not observed for $48f$, as this was above the upper-frequency limit of the active quadrupler. Neither up nor down transitions were observed for $55f$. This is discussed in the text.

n	$nf \rightarrow (n+1)k$ (GHz)	$nf \rightarrow (n-1)k$ (GHz)
48	58.55	
49	55.19	56.88
50	51.92	53.46
51	48.92	50.40
52	46.21	47.46
53	43.68	44.78
54	41.35	42.31
55		
56	37.04	37.84
57	35.20	35.99
58	33.33	34.06
59	31.77	32.38
60	30.21	30.76
61	28.71	29.24

Scanning the laser frequency, with the microwave frequency set to either one of these resonances shows enhancement of the same Rydberg state [Figs. 8(a) and 8(b)]. However, setting the microwaves at a frequency between those two resonances leads to no enhancement of the field-ionization signal [Fig. 8(c)]. Since the f-series quantum defect is approximately $\delta_f = 0.010$,[4] and the g-state quantum defect is estimated to be $\delta_g = 0.003$ (see Table I), we might reasonably assign these transitions to $51f$-$52g$ and $51f$-$50g$, since they are expected to appear at 48.54 and 50.76 GHz, respectively (referred to as the "up" and "down" transitions in what follows). The $51f$-state lifetime is 16 ns,[4] whereas the $50g$- and $52g$-state lifetimes are on the order of 1 μs.[17] Thus microwave frequencies resonant with these transitions would be expected to show enhancement of the Rydberg state signal observed by a field ionization pulse applied 750 ns after photoexcitation.

This situation is quite analogous to work performed with atoms.[31] In this case, optically excited low-l states would radiatively decay before the application of a field-ionization pulse, had they not been transferred to a longer-lived, higher-l state by a microwave field.

Analogous enhancement was observed by initially exciting the $48f$ to $54f$ and $56f$ to $61f$ states (the $55f$ state was a exceptional case, and will be discussed below). In all cases, both the up and down transitions were observed, with the frequencies of the observed resonances summarized in Table II.

In principle, the spectroscopic data summarized in Table II can be used to determine the quantum defects of the f series. If one assumes that states differing in n by 2 have the same quantum defect, this quantum defect may be determined by adding the nf-$(n+1)k$ and $(n+2)f$-$(n+1)k$ transition energies, and comparing the result to the hydrogenic spacing between n and $n+2$. Alternatively, up/down transitions beginning at the same n could be used to determine the quantum defect of the states we are exciting from the nf states. In practice, the observed resonances are too broad and the uncertainties in line centers too large to allow a precise determination of these quantities.

The widths of the observed resonances should reflect the nf-series lifetimes. However, at $n=51$ the expected full

width at half maximum (FWHM) is 10 MHz, whereas the observed resonances were much broader: the FWHM's of the resonances observed in Fig. 8(c) are 200 MHz. In addition, instead of a decrease in width with n, as would be expected due to the the n^{-3} scaling of the predissociation rates, the observed spectra have widths that increase with n. At $n=48$ the FWHM was roughly 160 MHz, and at $n=61$ the FWHM was 425 MHz.

Stray electric fields in the apparatus, and the microwave field itself will contribute to the observed width. Since the g series has an estimated quantum defect of 0.003 at $n=50$, an electric field of only 30 mV/cm will cause it to meet the manifold. Once the g state begins to interact with the manifold, Stark states become accessible by a single dipole coupling from the f state. This will broaden the observed lines. In Table II, where the observed up/down frequencies are tabulated, this uncertainty is denoted by labeling the final state in the observed transitions as nk.

It is also possible that interactions with background ions play a role in the observed widths, as demonstrated in the millimeter wave Rydberg state spectroscopy of Osterwalder and Merkt.[32] For example, although the $51f$-state lifetime is 16 ns, we still see a small amount of signal at this excitation energy even in the absence of a deliberately applied dc field. We expect that by paying careful attention to the ion density, microwave power used, and the cancellation of stray fields, as was done by Osterwalder and Merkt,[32] we could improve the experimental linewidths, and possibly obtain lifetime measurements of the nf series.

We were not able to observe stabilizing transitions from the $55f$ ($N^+=2$) state. In their time-resolved measurements of Rydberg state lifetimes, Vrakking and Lee[4] observed that the $55f$ ($N^+=2$) state had a significantly shorter lifetime than the states of adjacent n: 3.4 ns versus 25 ns. It is uncertain what nearby perturber is responsible for this shorter lifetime. However, this shorter lifetime is undoubtedly what limits our ability to stabilize this state.

VI. CONCLUSIONS AND FUTURE DIRECTIONS

Although this study was limited to NO, the techniques described will also allow the suppression of predissociation in other molecules. As was emphasized in the Introduction, the possibility of predissociation complicates the study of molecular Rydberg states below the first ionization threshold. In addition, both atoms and molecules have Rydberg states above the first ionization threshold that may autoionize. This is often an efficient nonradiative decay mechanism. These techniques are also directly applicable to autoionizing systems, since the goal is the same: transfer from an optically accessible low-l state to a high-l state that does not interact with the core. For example, the nd' Rydberg series approaching the second spin-orbit state of the Xe ion ($^2P_{1/2}$) rapidly autoionizes.[33] The autoionization rate is $1.0/(2\pi n^3)$. This is given in atomic units, and in a form emphasizing its size relative to the Kepler frequency—in this case, they are virtually identical. In contrast, the most rapidly decaying Rydberg series of NO has a predissociation rate of $1/\tau_p = 0.046/(2\pi n^3)$ (see Table I). As Held $et\ al.$[33] have shown, the spin-orbit autoionization of Xe provides a more demanding test of stabilization. However, Chupka[3] points out that the predissociation rates of NO are typical for small molecules, so the results obtained here should be generally applicable to molecular Rydberg states.

Recently Hofstein, Goode, and Johnson[34] have compared the Rydberg state survival probabilities of several small molecules: HCl, C_6H_6, N_2, and O_2 under conditions appropriate for photoinduced Rydberg ionization (PIRI) spectroscopy.[35] PIRI is a sensitive technique for ion spectroscopy, similar to the isolated core excitation method (ICE),[20,36] which relies on populating a Rydberg state converging on the ground state of an ion, then measuring laser-induced transitions of the ion core by detecting electrons from autoionization. This is a subtle process, since the Rydberg electron must not interact so much with the core that predissociation occurs before the the second excitation step, yet it must interact enough to allow autoionization to occur after core excitation. As Hofstein, Goode, and Johnson[34] point out, techniques for stabilization of lower-n Rydberg states could greatly enhance possible applications of PIRI. For example, any of the stabilization techniques presented in this paper could be applied during photoexcitation of the Rydberg state (for the techniques using a dc field, it would probably be wise to turn this off following initial excitation). After the ion-core transition step, the Rydberg electron could be forced to interact with the core by applying a large static field $[F>1/(3n^5)]$. If a core transition had been induced, the molecule would autoionize, yielding an electron for detection.

It is also of interest to extend the techniques of this paper to the lowest-n possible. A detection scheme which was sensitive to $n\to n+1$ transitions (selective field ionization,[20] for example) could then be used to detect either $n\,l\to n\pm1\ l\pm1$ single-photon transitions, or multiphoton transitions, as has been demonstrated by Osterwalder $et\ al.$[6,7] At low n and high l these would provide a sensitive probe of the electrical properties of the ionic core, free from the influence of weak stray electric fields.

[1] M. J. J. Vrakking, J. Chem. Phys. **105**, 7336 (1996).
[2] H. A. Bethe and E. E. Salpeter, *Quantum Mechanics of One- and Two-Electron Atoms* (Springer, Berlin, 1957).
[3] W. A. Chupka, J. Chem. Phys. **98**, 4520 (1993).
[4] M. J. J. Vrakking and Y. T. Lee, J. Chem. Phys. **102**, 8818 (1995).
[5] W. G. Sturrus, E. A. Hessels, P. W. Arcuni, and S. R. Lundeen, Phys. Rev. A **44**, 3032 (1991).
[6] A. Osterwalder, R. Seiler, and F. Merkt, J. Chem. Phys. **113**, 7939 (2000).
[7] A. Osterwalder and F. Merkt, Comments At. Mol. Phys. (unpublished).
[8] E. Murgu, J. D. D. Martin, and T. F. Gallagher, J. Chem. Phys. **113**, 1321 (2000).
[9] K. Müller-Dethlefs and E. W. Schlag, Annu. Rev. Phys. Chem. **42**, 109 (1991).
[10] E. W. Schlag, *ZEKE Spectroscopy* (Cambridge University Press, Cambridge, 1998).
[11] G. Reiser, W. Habenicht, K. Müller-Dethlefs, and E. W. Schlag, Chem. Phys. Lett. **152**, 119 (1988).
[12] G. Reiser and K. Müller-Dethlefs, J. Phys. Chem. **96**, 9 (1992).
[13] S. T. Pratt, J. Chem. Phys. **98**, 9241 (1993).
[14] A. Held, L. Y. Baranov, H. L. Selzle, and E. W. Schlag, Chem. Phys. Lett. **291**, 318 (1998).
[15] S. N. Dixit, D. L. Lynch, V. McKoy, and W. M. Huo, Phys. Rev. A **32**, 1267 (1985).
[16] M. Bixon and J. Jortner, J. Chem. Phys. **105**, 1363 (1996).
[17] A. Fujii and N. Morita, J. Chem. Phys. **103**, 6029 (1995).
[18] M. Y. Ivanov and A. Stolow, Chem. Phys. Lett. **265**, 231 (1997).
[19] P. Bellomo and C. R. Stroud, Jr., J. Chem. Phys. **110**, 7658 (1999).
[20] T. F. Gallagher, *Rydberg Atoms* (Cambridge University Press, Cambridge, 1994).
[21] R. Engleman, Jr., P. E. Rouse, H. M. Peek, and V. D. Baiamonte, Technical Report No. LA-4364, Los Alamos Scientific Laboratory, Los Alamos, NM (unpublished).
[22] N. J. Dovichi, D. S. Moore, and R. A. Keller, Appl. Opt. **21**, 1468 (1982).
[23] D. T. Biernacki, S. D. Colson, and E. E. Eyler, J. Chem. Phys. **89**, 2599 (1988).
[24] M. J. J. Vrakking (private communication).
[25] D. L. Albritton, A. L. Schmeltekopf, and R. N. Zare, J. Chem. Phys. **71**, 3271 (1979).
[26] V. Klimenko and T. F. Gallagher, Phys. Rev. Lett. **85**, 3357 (2000).
[27] P. M. Koch and K. A. H. van Leeuwen, Phys. Rep. **255**, 289 (1995).
[28] P. Pillet, H. B. van Linden van den Heuvell, W. W. Smith, R. Kachru, N. H. Tran, and T. F. Gallagher, Phys. Rev. A **30**, 280 (1984).
[29] J. R. Rubbmark, M. M. Kash, M. G. Littman, and D. Kleppner, Phys. Rev. A **23**, 3107 (1981).
[30] W. M. Griffith, M. W. Noel, and T. F. Gallagher, Phys. Rev. A **57**, 3698 (1998).
[31] K. A. Safinya, T. F. Gallagher, and W. Sandner, Phys. Rev. A **22**, 2672 (1980).
[32] A. Osterwalder and F. Merkt, Phys. Rev. Lett. **82**, 1831 (1999).
[33] A. Held, U. Aigner, L. Y. Baranov, H. L. Selzle, and E. W. Schlag, Chem. Phys. Lett. **299**, 110 (1999).
[34] J. D. Hofstein, J. G. Goode, and P. M. Johnson, Chem. Phys. Lett. **301**, 121 (1999).
[35] D. P. Taylor, J. G. Goode, J. E. LeClaire, and P. M. Johnson, J. Chem. Phys. **103**, 6293 (1995).
[36] W. E. Cooke, T. F. Gallagher, S. A. Edelstein, and R. M. Hill, Phys. Rev. Lett. **40**, 178 (1978).
[37] C. Jungen and E. Miescher, Can. J. Phys. **47**, 1769 (1969).
[38] E. Miescher, Can. J. Phys. **54**, 2074 (1976).
[39] M. L. Zimmerman, M. G. Littman, M. M. Kash, and D. Kleppner, Phys. Rev. A **20**, 2251 (1979).